Jordan Journal of Civil Engineering, Volume **20**, No. **3**, **2026**
DOI: https://doi.org/10.14525/JJCE.v20i3.02

Jordan Journal of Civil Engineering

Journal homepage: https://jjce.just.edu.jo

Predicting Chloride Corrosion Onset in Reinforced Concrete Structures Using Finite Element Method for Two-Dimensional Corrosion Problem

Tri N. M. Nguyen [1)], ***Xuan Tung Nguyen*** [2)*]

[1)] *Faculty of Civil Engineering, Industrial University of Ho Chi Minh City, Vietnam.*
[2)] *Faculty of Civil Engineering, Campus in Ho Chi Minh City, University of Transport and Communications, Vietnam.*
** Corresponding Author. Email: tungnx_ph@utc.edu.vn*

ARTICLE INFO

Article History:
Received: 11/7/2025
Accepted: 12/12/2025

ABSTRACT

One of the main reasons for damage and shortened service life in reinforced concrete (RC) structures, particularly in abrasive coastal conditions, is chloride-induced rebar corrosion. Accurately predicting the onset of corrosion is crucial for assessing structural reliability and planning effective maintenance. This paper proposes a finite element model to predict the onset of corrosion for a two-dimensional diffusion problem. The model is based on Fick's Second Law of Diffusion and employs the weighted Galerkin residual method to solve the partial differential equation. Parameters influencing the diffusion process and the chloride threshold concentration for corrosion are analyzed in detail. A computational program is developed using Matlab code, utilizing bilinear rectangular elements, to simulate chloride ion ingress and determine the onset of corrosion. The calculated results from the model are compared with the Life365 program, showing acceptable reliability, particularly under saturated humidity conditions. The study also analyzes the influences of material, environmental, and structural parameters on the onset of corrosion. Finally, the proposed model has significant implications for infrastructure asset management, enabling predictive maintenance planning, optimizing life-cycle costs, and enhancing structural service life.

Keywords: Chloride corrosion, RC durability, Corrosion initiation prediction, Finite element analysis.

INTRODUCTION

The corrosion of steel reinforcement is recognized as a major contributor to the deterioration of reinforced concrete (RC) structures. This process is primarily initiated by the penetration of aggressive substances from the surrounding environment, including carbon dioxide (CO_2), sulphate ions (SO_4^{2-}), and, most critically, chloride ions (Cl^-), which accelerate the onset and progression of corrosion within the concrete matrix (Topçu et al., 2022). These ions penetrate into the concrete through its porous structure or small cracks that develop due to drying shrinkage or temperature changes (Sannasiraj et al., 2025). The presence of chloride ions causes the neutralization of the passive film protecting the rebar. When the Cl^- ion concentration reaches the corrosion threshold, it alters the electro-chemical environment and causes passive film breakdown. Once the passive layer is destroyed, the rebar can begin to corrode if sufficient moisture and oxygen are supplied. This is an electro-chemical process with reactions occurring in anodic and cathodic regions. This electro-chemical reaction leads to the gradual dissolution of the anode, thereby reducing the cross-sectional area of the

reinforcing steel (Borg et al., 2017; Mundra et al., 2017). This process results in the dissolution of iron at the anode and the formation of corrosion products. These products occupy 2 to 6.5 times the volume of the original steel, creating expansive internal pressures that cause cracking, spalling, and delamination of the concrete cover. Furthermore, the corrosion process reduces the effective cross-sectional area and strength of the rebar, directly affecting both the load-bearing capacity and the overall performance of the RC component (Fuhaid & Niaz, 2022, Hu et al., 2022, Bidari et al., 2024). The dual degradation of both the steel and the concrete underscores the seriousness of chloride corrosion as a structural safety and serviceability concern.

Predicting the onset of chloride-induced corrosion primarily relies on modeling the diffusion of chloride ions from the surface into the concrete. According to Fick's Second Law, chloride transport is governed by a concentration gradient. Corrosion initiation is assumed to occur when the chloride concentration at the reinforcement surface surpasses a critical threshold. Angst (2019) demonstrated that threshold-based models remain the only available approach, yet their reliability is limited when applied to field data, owing to variability in critical chloride levels obtained from laboratory specimens versus in-situ concrete core specimens. Furthermore, Peng et al. (2020) underscored the importance of accounting for the spatio–temporal variability of the diffusion coefficient and material and environmental parameters when forecasting service life and durability under chloride exposure. Employing a spatio-temporal probabilistic framework enhances corrosion-risk assessment and supports resilient structural design. Slika and Saad (2016) confirmed that integrating numerical models with real-time sensor data and the Ensemble Kalman Filter technique offers a powerful methodology for accurately predicting chloride-induced corrosion initiation, thereby enabling proactive maintenance and extending structural service life. In addition, Wu et al. (2020) demonstrated that their two-dimensional chloride diffusion model in concrete demonstrated improved accuracy in forecasting both service life and corrosion risk in actual structural elements.

However, accurately modeling this diffusion is exceptionally complex. The concrete's transport properties are not constant; they are highly dependent on the mix design. An experimental study by Assas (2012) demonstrated that the water-cement (w/c) ratio and the inclusion of pozzolanic admixtures, like Silica Fume (SF) and Fly Ash (FA), significantly alter the concrete's resistance to chloride ion permeability. He found that silica fume, in particular, was highly effective in reducing permeability and enhancing durability compared to normal concrete. Thus, while numerous numerical schemes exist, this study presents an alternative solution using a Galerkin weighted-residual formulation within the FEM. Although analytical solutions are available for 1D problems involving constant parameters, the finite element method becomes essential for addressing the 2D problem, as it must incorporate the time-dependent nature of diffusion and the critical influence of material parameters, including admixtures (SF, FA) and environmental humidity, which are essential for realistic service life assessment. The calculated results will be benchmarked against the Life365 software to verify their reliability. In summary, this model will serve as a support tool for engineers and managers in guiding timely maintenance, repair strategies, or the selection of more durable materials for coastal structures, ultimately prolonging the service life of the structure.

Theoretical Background and Methodology

Chloride Diffusion into Concrete

Models describing chloride ion diffusion into concrete are commonly based on Fick's laws of diffusion. This is the direct mathematical foundation for non-steady-state diffusion modeling. For a two-dimensional (2D) problem:

$$\frac{\partial C(x,y,t)}{\partial t} = \frac{\partial}{\partial x}\left(D\frac{\partial C(x,y,t)}{\partial x}\right) + \frac{\partial}{\partial y}\left(D\frac{\partial C(x,y,t)}{\partial y}\right) \quad (1)$$

where $C(x,y,t)$ is the chloride concentration at location (x, y) and time t (% by concrete mass), D is the chloride diffusion coefficient in concrete (m^2/s), x, y are distances from the concrete surfaces (m), and t is time (years).

Apparent Chloride Diffusion Coefficient (D_a) and Influencing Parameters

The apparent chloride diffusion coefficient (D_a) is a non-steady-state quantity that depends on material composition, time, and environmental humidity. Studies have shown that D_a can significantly decrease with

concrete age due to ongoing cement hydration reactions, which partially fill the pore system (Song et al., 2013; Zhou et al., 2019; Xu et al., 2024). The general formula for predicting D_a is determined as:

$$D_a = D_{28} . f_{SF} . f_t . f_T . f_H + \frac{W_{cr}}{S_{cr}} D_{cr} \quad (2)$$

The parameters influencing D_a include:

Diffusion coefficient at 28 days (D_{28}): Depends on the water-cement ratio (w/c) (Thomas & Bentz, 2002).

$$D_{28} = 10^{(-12.06+2.4 w/c)} \ (m^2/s) \quad (3)$$

Effect of silica fume (f_{SF}): The empirical formula for this effect is:

$$f_{SF} = e^{-0.165 SF} \quad (4)$$

where SF is the percentage of SF in concrete. This relationship is recommended when the SF content is less than 15%.

Effect of time (f_t): The diffusion coefficient decreases with concrete age. This relationship is expressed by an exponential function:

$$f_t = \left(\frac{t_{28}}{t}\right)^m \quad (5)$$

where t is the concrete age (years), the constant m depends on the mix proportion, and the admixture, such as SG, FA:

$$m = 0.2 + 0.4 \left(\frac{\%FA}{50} + \frac{\%SG}{70}\right). \quad (6)$$

To prevent an unrealistic continuous decline, the proposed relationship for the diffusion coefficient is applied only up to 25 years. Then, the diffusion coefficient is maintained at its 25-year value for the remainder of the service life assessment.

Effect of temperature (f_T): Based on the Arrhenius equation, the relationship between the chloride diffusion coefficient and temperature is described by:

$$f_T = exp\left[\frac{U}{R}\left(\frac{1}{T_{ref}} - \frac{1}{T}\right)\right] \quad (7)$$

where U = 35,000 (J/mol), is the activation energy for diffusion; R = 8.314 ($JK^{-1}mol^{-1}$), is the gas constant; T is the ambient temperature (K); and T_{ref} = 273K.

Effect of humidity (f_H): The diffusion coefficient is accounted for by combining synthetic theories with Powers' model (Saetta et al., 1993):

$$f_H = \left[1 + \left(\frac{1-H}{1-H_C}\right)^4\right]^{-1} \quad (8)$$

where H is the environmental humidity in %; H_c = 75%.

Effect of cracks: Cracks create pathways for chloride ingress, increasing the diffusion coefficient. This effect is calculated by Boulfiza et al. (2003) as:

$$D_a = D_c + D_{cr} \frac{W_{cr}}{S_{cr}} \quad (9)$$

where D_c denotes the chloride diffusion coefficient in uncracked concrete, w_{cr} denotes the crack width (mm), and s_{cr} denotes the spacing between cracks. D_{cr} = 5.10^{-10} m^2/s and the value of w_{cr}/s_{cr} is typically 3.10^{-4} (Boulfiza et al., 2003).

Critical Chloride Threshold Concentration (C_{th})

The critical threshold concentration (C_{th}) is the chloride content at the reinforcement steel surface required to break down the passive film and initiate corrosion (Lawler et al., 2021). Literature review showed various standards that set maximum chloride contents (usually as a percentage of cementitious material) to protect embedded steel. Table summarizes current limits from codes and guidelines.

Table 1. Summary of standards for maximum permissible chloride limits

Standard/Source	Material/Component	Max. Cl^- Limit (% of cement)	Cl^- form	Notes (Exposure, Comments)
ACI 318-19 (USA)	RC (carbon steel)	0.15 (C2); 0.30 (C1); 1.00 (C0)	Water-soluble	C2 (wet+salt); C1 (moisture); C0 (dry)

	Pre-stressed concrete	0.06	Water-soluble	All exposure classes (water-soluble Cl^-)
PTI M55.1 (USA)	Grout (post-tensioning)	0.08	Total (acid-soluble)	(ASTM C1152 testing)
BS 8500-1:2023 (EU/UK)	RC (carbon steel)	0.40	Total (acid-soluble)	Chloride class Cl
	Pre-stressed concrete (pre-tensioned)	0.10	Total (acid-soluble)	Chloride class Cl
EN 447 (EU)	Pre-stressed tendon grout	0.10	Total (acid-soluble)	EN 447 basic requirement for tendon grout
CSA A23.1/A23.2 (Canada)	Pre-stressed concrete	0.06	Water-soluble	(Clause 4.1.1.2) same as ACI 318
NZRMCA (New Zealand)	Pre-stressed concrete	0.14	Total (acid-soluble)	Maximum 0.5 kg/m³ chloride
JPCEA (Japan)	Tendon grout	0.023	Total (acid-soluble)	0.3 kg/m³
Hong Kong CoP (HK)	Pre-stressed concrete	0.10	Total (acid-soluble)	(Pre-cast Concrete Code)
FDOT Spec 934 (Florida, USA)	Cast-in-place concrete	0.067	Total (acid-soluble)	0.40 lb/yd³

Table 1 indicates that there is no single "universal" C_{th} value. Based on the analyses and for simplification purposes of this study, the authors recommend using C_{th}=0.05% by concrete mass for ordinary RC.

Finite Element Model for Predicting Corrosion Onset

Concept of Service Life and the Onset of Corrosion

The service life of a structure is the period from construction until a certain limit state is violated. For RC bridge structures exposed to marine environment, service life is defined as the time from initial exposure to a chloride-containing environment until chloride-induced rebar corrosion. In the classic two-phase model (Tuutti's model), service life is divided into: (1) *onset* – the time until chlorides break passivity (t_1) – and (2) *propagation* – the time from initiation to visible damage (t_2) (Tuutti, 1980; Lawler et al., 2021). Corrosion is assumed to initiate when the chloride concentration at the bar surface exceeds C_{th}. Thus, the onset of corrosion depends on chloride exposure, diffusion through cover, cover depth, and the threshold value. Once onset of corrosion occurs, service-life models track corrosion rate and cover cracking until failure. Within the scope of this study, the research focuses only on calculating and predicting the onset of corrosion (t_1).

Model for Predicting the Onset of Corrosion

Model Parameters

Predicting the onset of corrosion is based on the diffusion of chloride ions. The corrosion onset will end when the chloride concentration at the rebar surface reaches the corrosion threshold concentration.

The model for predicting the onset of corrosion is based on Fick's Second Law of diffusion. For a 2D problem (for beams and columns) (Refer to Eq. (1)):

$$\frac{\partial C(x,y,t)}{\partial t} = \frac{\partial}{\partial x}\left(D\frac{\partial C(x,y,t)}{\partial x}\right) + \frac{\partial}{\partial y}\left(D\frac{\partial C(x,y,t)}{\partial y}\right). \quad (1)$$

In practice, both the diffusion coefficient D and the surface chloride concentration C change over time. Therefore, to solve this problem, the weighted Galerkin residual method within the finite element method is used.

The input parameters in the problem are crucial to ensure the accuracy of the model.

Chloride Diffusion Coefficient (D_a): Refer to Eq. (2).

Chloride Accumulation on Concrete Surface ($C_s(t)$): According to Michael Thomas - Life 365, $C_s(t)$ changes linearly with time depending on the region:

$$C_s(t)=\begin{cases} kt \quad ,t\leq\frac{C_{s,max}}{k} \\ C_{s,max} \quad , t\geq\frac{C_{s,max}}{k} \end{cases} \tag{10}$$

where k is the accumulation rate (%/year) and $C_{s,max}$ is the maximum chloride concentration on the surface (%/concrete mass). These values are given in Table 2.

Table 2. Values of k and $C_{s,max}$

Region	***k* (%/year)**	***C*$_{s,max}$ (%/concrete mass)**
Tidal zone	Occurs on day 0.8	0.8
Splash zone	0.10	1.0
≤800m	0.04	0.6
800m to 1500m	0.02	0.6

Chloride Thresholds Concentration (C_{th}):
C_{th}= 0.05%.

Developing the Finite Element Equation for Predicting the Onset of Corrosion

Galerkin Method

To solve the partial differential equation of Fick's Second Law Eq. (1), the weighted Galerkin residual method is applied. The general form of the diffusion equation is:

$$\frac{\partial \emptyset}{\partial \mathrm{t}}+\frac{\partial \mathrm{J_x}}{\partial \mathrm{x}}+\frac{\partial \mathrm{J_y}}{\partial \mathrm{y}}=0 \tag{11}$$

where ϕ is the chloride concentration $C(x,y,t)$, and J_x, J_y are the chloride fluxes in the x, y directions. Applying the Galerkin method, the equation is multiplied by a weighting function $W(x,y)$ and integrated over the computational domain Ω:

$$\int_{\Omega} \mathrm{W}\left(\frac{\partial \emptyset}{\partial \mathrm{t}}+\frac{\partial \mathrm{J_x}}{\partial \mathrm{x}}+\frac{\partial \mathrm{J_y}}{\partial \mathrm{y}}\right) \mathrm{d}\Omega = 0. \tag{12}$$

The domain Ω is divided into elements, and the field variable ϕ within each element is approximated by nodal values and interpolation (shape) functions:

$$\phi^{(e)}=[N]\{\Phi\}^{(e)} \tag{13}$$

In the Galerkin method, the weighting functions W_i are chosen to be the shape functions N_i of the element. After applying integration by parts (Green's theorem) to reduce the order of spatial derivatives, the element-level equation takes the following matrix form:

$$[C]^{(e)}\{\dot{\Phi}\}^{(e)}+[K]^{(e)}\{\Phi\}^{(e)}=\{I\}^{(e)} \tag{14}$$

where:

- $[C]^{(e)}$ is the element capacitance matrix, representing the element's ability to accumulate chloride.
- $[K]^{(e)}$ is the element characteristic matrix, representing the element's diffusion capability.
- $\{I\}^{(e)}$ is the element integral vector, representing chloride flux across the element boundary.

The Galerkin method links continuous differential equations with discrete algebraic systems, enabling the numerical solution of complex problems without analytical solutions. It also supports modeling irregular geometries and boundary conditions.

Description of Bilinear Rectangular Element

To discretize the computational domain, especially for two-dimensional problems (beams and columns), the bilinear rectangular element is used. With a length of 2b along the x-axis and a width of 2a along the y-axis (Figure), the field variable ϕ within the element is described by:

$$\phi^{(e)}=N_i\Phi_i+N_j\Phi_j+N_k\Phi_k+N_l\Phi_l \tag{15}$$

where N_i, N_j, N_k, N_l are the shape functions associated with nodes i, j, k, l, respectively, and Φ_i, Φ_j, Φ_k, Φ_l represent the corresponding nodal values of the scalar field ϕ. For a rectangular finite element defined in a local coordinate system x′−y′, with the origin located at node i, the shape functions are defined by Equations (16) to (19).

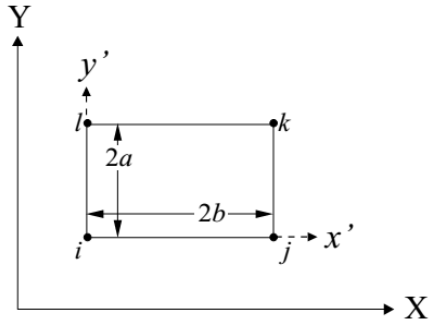

Figure 1. Bilinear rectangular element

$$N_i = \left(1 - \frac{x'}{2b}\right)\left(1 - \frac{y'}{2a}\right) \tag{16}$$

$$N_j = \frac{x'}{2b}\left(1 - \frac{y'}{2a}\right) \tag{17}$$

$$N_k = \frac{x'y'}{4ab} \tag{18}$$

$$N_j = \frac{y'}{2a}\left(1 - \frac{x'}{2b}\right) \tag{19}$$

Estimation of Element Integrals

The integrals for the capacitance matrix, characteristic matrix, and environmental load vector are estimated using the shape functions of the bilinear rectangular element

Capacitance Matrix ($[C]^{(e)}$):

$$[C] = \frac{\kappa ab}{9}\begin{bmatrix} 4 & 2 & 1 & 2 \\ & 4 & 2 & 1 \\ & & 4 & 2 \\ sym & & & 2 \end{bmatrix} \tag{20}$$

where 2a,2b are the height and width of the rectangle, and κ=1/D.

Characteristic Matrix ($[K]^{(e)}$):

$$[K]^{(e)} = \frac{1}{6ab}\begin{bmatrix} 2(a^2+b^2) & (b^2-2a^2) & -(a^2+b^2) & a^2-2b^2 \\ & 2(a^2+b^2) & a^2-2b^2 & -(a^2+b^2) \\ & & 2(a^2+b^2) & (b^2-2a^2) \\ sym & & & 2(a^2+b^2) \end{bmatrix} \tag{21}$$

Environmental Load Vector ($\{f\}^{(e)}$):

$$\{f\}^e = \frac{C_{s(t)}}{2}\begin{Bmatrix} l_{ij}+l_{il} \\ l_{ij}+l_{jk} \\ l_{jk}+l_{kl} \\ l_{kl}+l_{il} \end{Bmatrix} \tag{22}$$

This equation applies only to the sides of the rectangle where chloride flux is defined, with l_{ij}, l_{jk}, l_{kl}, l_{il} being the lengths of the corresponding sides.

The explicit formulae for the capacitance matrix, characteristic matrix, and environmental load vector are the fundamental "building blocks" of the FEM model. The accuracy of these matrices determines the accuracy of the entire model.

Algorithm for Time-dependent Two-dimensional Chloride Diffusion Problem

After assembling the element matrices using the direct stiffness method, a system of linear first-order differential equations with respect to time is obtained as:

$$[C]\{\dot{\Phi}\} + [K]\{\Phi\} - \{f\} = 0 \tag{23}$$

To obtain a numerical solution, this equation is solved over time using a Crank-Nicolson finite difference approximation:

$$\left(\frac{2}{\Delta t}[C] + [K]\right)\{\Phi\}_{t+\Delta t} = \left(\frac{2}{\Delta t}[C] - [K]\right)\{\Phi\}_t + \{F\}_t + \{F\}_{t+\Delta t}. \tag{24}$$

This equation estimates the chloride concentration at time $(t+\Delta t)$ based on the value at the previous time step t.

The computational program to solve the two-dimensional diffusion equation has been written using Matlab software. The program uses bilinear rectangular elements, with the capacitance matrix, characteristic matrix, and environmental load vector calculated from Equations (20), (21), (22) as presented. The program structure includes a main script that controls the computation process and calls specialized sub-functions to perform specific tasks (Figure 2).

The computational algorithm used to solve the time-

dependent two-dimensional chloride diffusion is illustrated in Figure 2.

1. Input parameters: Including the geometric shape of the structure (concrete cover thickness L_x, L_y), material properties (water/cement ratio, admixtures SF, FA, SG, temperature T, humidity H), chloride threshold concentration, boundary and initial conditions.
2. During the initiation stage (time loop):
   a. Solve for chloride concentration C(x,y,t) at each time step using Eq. (24).
   b. Check termination condition: If the chloride concentration at the rebar surface (e.g. at node 25 in the 2D model) reaches the threshold concentration (C_{th} = 0.05%), corrosion is assumed to begin, and the calculation stops. The program will output the corrosion initiation time (t_I). Otherwise, time is incremented by a time step Δt =12 hours (in years) and step 2 is repeated.

Specific Boundary Conditions and Initial Conditions for the Two-dimensional Problem

- Boundary Conditions: Chloride concentration at boundary nodes exposed to the environment is set equal to the surface chloride concentration C_s *(t)*. Specifically, in the 2D model, the boundary nodes are:
  $\phi(1)=\phi(2)=\phi(3)=\phi(4)=\phi(5)=\phi(6)=\phi(11)=\phi(16)=\phi(21)=C_s(t)$, within the range $0\leq x\leq L_x$, $0\leq y\leq L_y$.
- Initial Conditions: At t = 0, diffusion has not occurred. Boundary nodes have a chloride concentration equal to C_s *(t)*, and chloride concentration at all other internal nodes is set to 0.
- Termination Condition: When the chloride concentration at node 25 (the node representing the rebar location) reaches the threshold C_{th} = 0.05 %, the problem stops, and the onset of corrosion is printed.

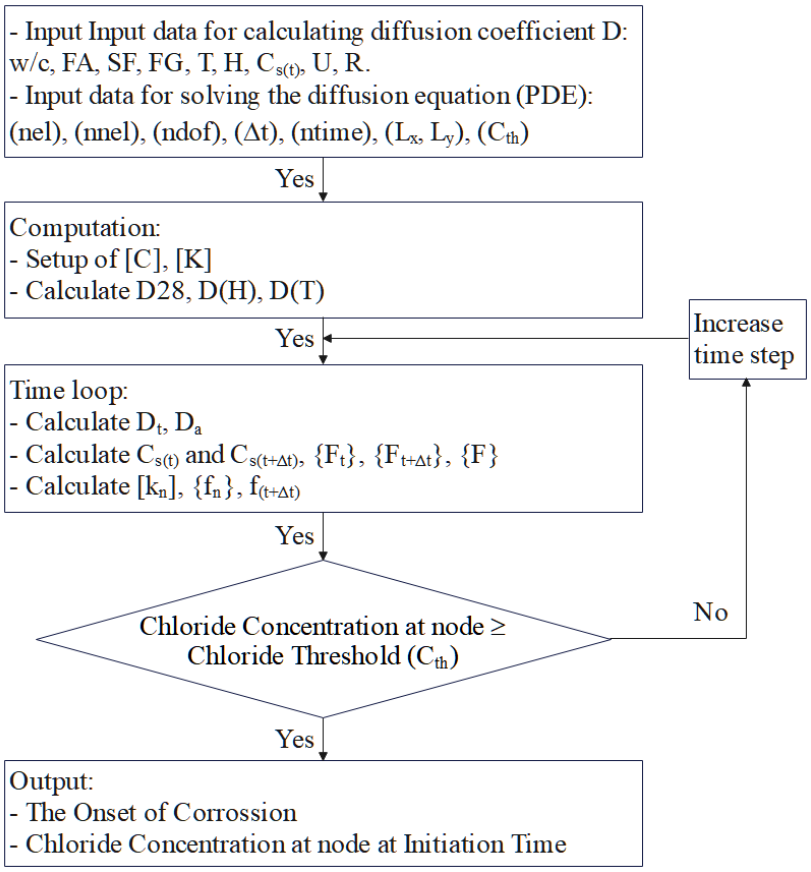

Figure 2. The algorithm for solving the time-dependent two-dimensional chloride diffusion

RESULTS AND DISCUSSION

Calculated Corrosion Initiation Time and Chloride Concentration Distribution

The model domain is discretized with 16 elements, resulting in a total of 25 nodes. The problem layout is illustrated in Figure 3.

Parameters of the Problem

Concrete cover thickness: $L_x = L_y = 0.07$ (m).
Water-to-cement ratio: w/c = 0.35.
Admixtures:
• FA = 0, 5, 8 (%).
• SG = 0.
• SF = 0, 5, 8 (%).
Humidity: H = 100%, 75%.
Time step: Δt = 12 hours.
Surface chloride concentration: $C_s(t) = 0.6$.
Critical chloride threshold: $C_{th} = 0.05$.

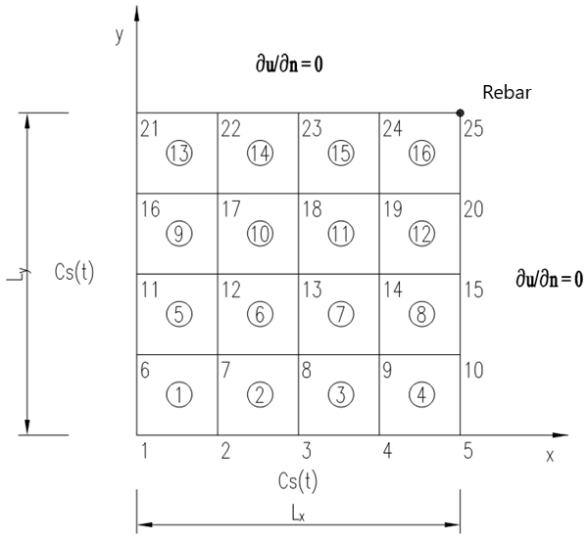

Figure 3. Schematic of the 2D chloride diffusion problem

The calculated results from the Matlab source code for the two-dimensional diffusion problem show that the onset of corrosion (t_1) is 16.6356 years. It should be noted that the final chloride concentration before reaching the critical threshold is 0.04.

The chloride concentration distribution at the nodes of the model after calculation (expressed as a 5x5 matrix for 25 nodes) is:

ans =

0.5994	0.3794	0.1570	0.0628	0.0400
0.5994	0.3866	0.1731	0.0841	0.0628
0.5995	0.4197	0.2434	0.1731	0.1570
0.5997	0.5075	0.4197	0.3866	0.3794
0.6000	0.5997	0.5995	0.5994	0.5994

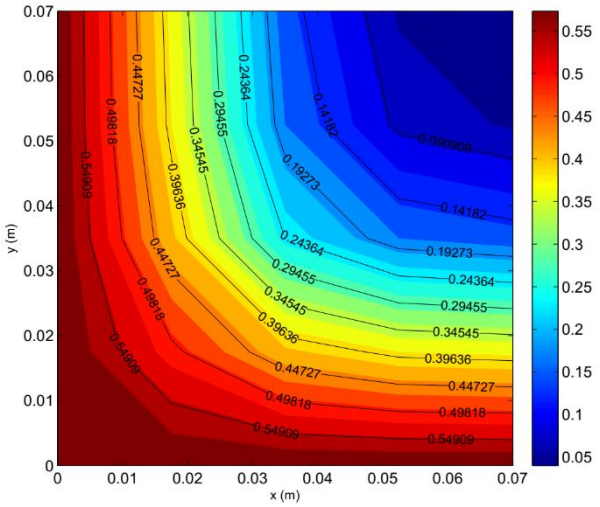

Figure 4. Chloride concentration contour plot at t_1

Figure 4 shows the chloride concentration distribution as a contour plot at the time of corrosion initiation (t_1 = 16.64 years). The plot clearly visualizes the 2D diffusion pattern, with the highest concentrations at the exposed boundaries (nodes 1-5 and 6, 11, 16, 21) and the concentration at the rebar location (node 25) reaching the threshold C_{th} = 0.05%. These observations represent the chloride concentration at each node in the finite element mesh, allowing for visualization of the concentration distribution along the depth and width of the component. The highest concentrations are at the boundary nodes exposed to the environment and gradually decrease inwards.

Comparison with Life365 Program and Discussion

Our validation was performed by benchmarking the proposed finite element model against the Life365 service life prediction program, which is a widely accepted industry standard for chloride ingress modeling. To ensure a valid "apples-to-apples" comparison, the following steps were taken: (1) Parameter Matching: Key input parameters, including water-cement ratio (w/c), concrete cover thickness, temperature (T), and critical chloride threshold (C_{th}), were set to identical values in both our FEM model and the Life365 program. (2) Condition Alignment: The

Life365 program, in its standard calculation, assumes fully saturated concrete humidity (H=100%). Therefore, for the specific purpose of validation, our proposed model was also run with the humidity parameter (f_H) set to H=100%.

The results of this direct comparison are presented in Table 3 and Figure 5. As shown, the corrosion onset times (t_1) predicted by our model under saturated conditions show good agreement with the outputs from Life365. This strong correlation validates the fundamental correctness of our finite element formulation and MATLAB implementation.

Table 3. Corrosion onset results by parameters - 2D problem

Concrete Cover Thickness (mm)	**w/c**	**SF(%)**	**FA(%)**	**D_{28}**	**T(K)**	**C_s**	**C_{th}**	**t_1 (years) Life365**	**t_1 (years) Proposed Model**
50	0.35	0	0	6.026	293(20)	0.6	0.05	9	9.3
40	0.35	0	0	6.026	293(20)	0.6	0.05	6.7	6.6
50	0.4	0	0	7.94	293(20)	0.6	0.05	7.5	7.5
50	0.35	0	0	6.026	295(22)	0.6	0.05	8.4	7.9
50	0.35	0	0	6.026	293(20)	0.6	0.04	8.2	8.5
50	0.35	5	0	2.64	293(20)	0.6	0.05	16.1	17.1
50	0.35	8	0	1.61	293(20)	0.6	0.05	23.7	26.5
50	0.35	0	5	6.026	293(20)	0.6	0.05	10.1	9.5
50	0.35	0	8	6.026	293(20)	0.6	0.05	10.8	10.2

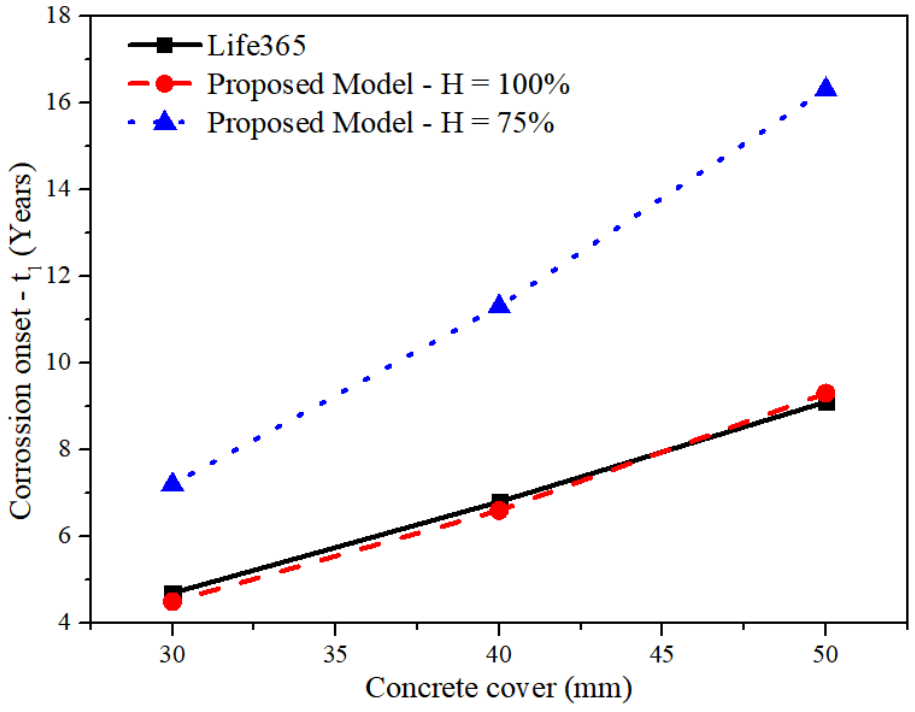

Figure 5. Comparison of corrosion onset for H = 100 % and H = 75 % - 2D problem

Figure 5 visualizes the comparison of corrosion onset time (t_1) at different concrete cover thicknesses (30, 40, and 50 mm) between the models. The x-axis represents concrete cover thickness, and the y-axis represents corrosion initiation time t_1. The corrosion onset from the proposed program shows minor discrepancies compared to that of the Life365 program when calculated with H=100%. However, there is a

larger discrepancy when calculated with H=75%. This is explained by the fact that the Life365 program always assumes saturated humidity (H=100%). When humidity is not saturated, the diffusion process slows down, leading to an increase in the onset of corrosion. The ability to calculate with unsaturated humidity is a significant advantage of the model, as unsaturated conditions are common in real RC components. This allows the model to provide more accurate predictions for actual scenarios.

Sensitivity Analysis of Parameter Influence on the Onset of Corrosion

Corrosion onset is influenced by three main groups of factors: material design, environmental factors, and structural design.

- **Regarding Material Design**

Water-to-cement ratio: When increasing the w/c ratio from 0.35 to 0.4 (Table 3), the corrosion onset decreases from 9.3 years to 7.5 years (for 50-mm thickness). This is because a higher *w/c* ratio increases the porosity of the concrete, leading to an increased chloride diffusion coefficient, and thus faster chloride ingress.

Admixtures: The addition of SF has a significant impact on extending the onset of corrosion. According to Table, increasing SF from 0 % to 5 % and 8 % (with w/c=0.35, 50mm thickness) increases the corrosion onset from 9.3 years to 17.1 years and 26.5 years, respectively. This is because SF significantly reduces the permeability and diffusion coefficient of concrete, slowing down chloride ingress. Although not as significant as SF, FA and SG also contribute to reducing the diffusion rate over time (through the constant m), thereby extending service life. This allows an engineer or asset manager to perform a direct cost-benefit analysis, weighing the higher initial material cost of SF against an extension in predicted service life.

- **Regarding Environmental Factors**

Temperature (T): When the temperature increases from 293K (20°C) to 295K (22°C) (Table 3), the corrosion onset decreases from 9.3 years to 7.9 years. This is consistent with the theory that higher temperatures increase the diffusion rate of chloride ions.

Surface chloride concentration (C_s): A higher *Cs* value leads to a larger concentration gradient, resulting in a faster diffusion rate and shorter corrosion onset.

Environmental humidity (H): As analyzed, humidity has a very significant influence. The model's most significant practical implication is its ability to account for non-saturated humidity (H < 100%). The findings show that reducing humidity from 100% to 75% for a 50-mm cover component nearly doubles its predicted service life (9.3 *vs.* 16.3 years) (Table 3). This is critically important, as it suggests that applying fully saturated models to components in drier micro-climates can lead to unnecessary expense and over-design.

- **Regarding Structural Design**

Concrete cover thickness: As the concrete cover thickness increases, the corrosion onset also significantly increases (Table 3 and Figure 4). For example, increasing the thickness from 30 mm to 50 mm (with H=100%) increases the corrosion initiation time from 4.5 years to 9.3 years. This is because chloride needs more time to diffuse through a thicker concrete layer to reach the rebar. Thus, the model allows for a more nuanced approach to design specifications than a simple prescriptive code. For instance, an engineer can compare the cost of increasing the concrete cover from 40-mm to 50-mm (which extends t_1 from 6.6 to 9.3 years) *versus* the cost of adding 5% FA (which extends t_1 from 9.3 years to 9.5 years, a minor change).

CONCLUSIONS

This study successfully developed and validated a finite element model to predict the initiation of chloride-induced corrosion in RC structures. The model, based on Fick's Second Law and the Galerkin weighted-residual method, solves a 2D time-dependent diffusion problem, capturing critical 'corner effects' that 1D models cannot.

A primary conclusion of this work is the substantial influence of environmental humidity on service life predictions. The study demonstrates that standard models assuming fully saturated conditions tend to yield overly conservative estimates. By accounting for non-saturated reality, the proposed model reveals that service life can be significantly extended in drier environments. Furthermore, the parametric analysis highlights the superior efficacy of mineral admixtures, particularly silica fume, in delaying corrosion initiation. The inclusion of such admixtures was found to provide a more effective improvement in durability compared to

solely increasing the concrete cover thickness.

Results showed good agreement with Life365 predictions under saturated conditions, validating the model's baseline accuracy. The proposed model thus offers a flexible and more realistic framework for durability-based design, service-life prediction, and maintenance planning in infrastructure management.

Future research directions should focus on three key areas: (1) extending the model to 3D to simulate more complex structural geometries; (2) experimental validation by comparing the model's predictions against laboratory-based corrosion data; and (3) developing a probabilistic framework (e.g. using Monte Carlo simulation) to quantify the uncertainty of input parameters and enable more reliable, non-deterministic service life predictions.

Acknowledgments

The authors acknowledge the Industrial University of Ho Chi Minh City (IUH).

REFERENCES

ACI CODE-318. (2022). *Building code requirements for structural concrete and commentary*. American Concrete Institute, USA.

ACI Committe 365. (2012). *Life-365 service life prediction model and computer program for predicting the service life and life-cycle cost of reinforced concrete exposed to chlorides (Version 2.1)*. American Concrete Institute.

Angst, U. M. (2019). Predicting the time to corrosion initiation in reinforced concrete structures exposed to chlorides. *Cement and Concrete Research, 115*, 559-567. https://doi.org/10.1016/j.cemconres.2018.08.007

Assas, M.M. (2012). Assessment of the transport properties and strength of concretes having different mix proportions, silica fume and fly ash additions. *Jordan Journal of Civil Engineering, 6*(3), 340-352.

ASTM. (2004). *Standard test method for acid-soluble chloride in mortar and concrete (ASTM C1152/C1152M-04)*. ASTM International.

Bidari, O., Singh, B. K., & Maheshwari, R. (2024). Effect of corrosion on bond between reinforcement and concrete: An experimental study. *Discover Civil Engineering, 1*(1), 67.

Borg, R. P., Gatt, E., & Sammut, S. (2017). Chloride ion detection in concrete through galvanic and resistivity methods. *Jordan Journal of Civil Engineering, 11*(4).

Boulfiza, M., Sakai, K., Banthia, N., & Yoshida, H. (2003). Prediction of chloride ions ingress in uncracked and cracked concrete. *ACI Materials Journal, 100*(1).

BSI. (2007). *BS EN 447:2007. Grout for prestressing tendons—Basic requirements*. BSI.

BSI. (2023). *BS 8500-1:2023. Concrete—Complementary British Standard to BS EN 206—Method of specifying and guidance for the specifier*. BSI.

Canadian Standards Association. (2009). *CSA A23.1-09: Concrete materials and methods of concrete construction (Section 4.1.1.2: Limits on chloride ion content)*. Canadian Standards Association.

Florida Department of Transportation. (2010). *Standard specifications for road and bridge construction*. Florida Department of Transportation.

Fuhaid, A.. F., & Niaz, A. (2022). Carbonation and corrosion problems in reinforced concrete structures. *Buildings, 12*.

Hong Kong Buildings Department. (2003). *Code of practice for precast concrete*. Hong Kong Buildings Department.

Hu, J.Y., Zhang, S.S., Chen, E., & Li, W.G. (2022). A review on corrosion detection and protection of existing reinforced concrete (RC) structures. *Construction and Building Materials, 325*, 126718.

Japan Prestressed Concrete Engineering Association. (2007). *Guidelines for design and construction of grouting for prestressed concrete structures (Vol. 1, Section 4.2, commentary)*. Japan Prestressed Concrete Engineering Association.

Lawler, J.S., Kurth, J.C., Garrett, S.M., & Krauss, P.D. (2021). Statistical distributions for chloride thresholds of reinforcing bars. *ACI Materials Journal, 118*(2).

Mundra, S., Criado, M., Bernal, S. A., & Provis, J.L. (2017). Chloride-induced corrosion of steel rebars in simulated pore solutions of alkali-activated concretes. *Cement and Concrete Research, 100*, 385-397. https://doi.org/10.1016/j.cemconres.2017.07.006

New Zealand Ready Mixed Concrete Association Inc. (2005). *Chloride content of fresh concrete*. New Zealand Ready Mixed Concrete Association Inc.

Saetta, A.V., Scotta, R.V., & Vitaliani, R.V. (1993). Analysis of chloride diffusion into partially saturated

concrete. *ACI Materials Journal*, *90*(5).

Sannasiraj, R.S.A., Shi, S., Liu, X., Gryllias, K., Vandepitte, D., Chronopoulos, D., & Zhang, L. (2025). A fully coupled depth-dependent corrosion model for reinforced concrete piles under marine environmental conditions. *Construction and Building Materials*, *472*, 140795.

Slika, W., & Saad, G. (2016). An ensemble Kalman filter approach for service life prediction of reinforced concrete structures subject to chloride-induced corrosion. *Construction and Building Materials*, *115*, 132-142. https://doi.org/10.1016/j.conbuildmat.2016.04.018

Song, L., Sun, W., & Gao, J. (2013). Time dependent chloride diffusion coefficient in concrete. *Journal of Wuhan University of Technology-Materials Science Edition*, *28*(2), 314–319.

Thomas, M., & Bentz, E. (2002). *Computer program for predicting the service life and life-cycle costs of reinforced concrete exposed to chlorides (Life365 manual)*, SFA.

Topçu, İ.B., Uzunömeroğlu, A., & Pat, S. (2022). Enhanced corrosion behavior of reinforcing steel in concrete using titanium nano-composite thin films. *Jordan Journal of Civil Engineering*, *16*(2).

Tuutti, K. (1980). Service life of structures with regard to corrosion of embedded steel. In *ACI Symposium Publication* (SP-65).

Wu, L., Wang, Y., Wang, Y., Ju, X., & Li, Q. (2020). Modelling of two-dimensional chloride diffusion concentrations considering the heterogeneity of concrete materials. *Construction and Building Materials*, *243*, 118213. https://doi.org/10.1016/j.conbuildmat.2020.118213

Xu, Q., Liu, B., Dai, L., Yao, M., & Pang, X. (2024). Factors influencing chloride ion diffusion in reinforced concrete structures. *Materials*, *17*.

Zhou, H., Zhou, X.-Z., Zhang, J., & Zheng, J.-J. (2019). Effective medium method for chloride diffusion coefficient of mature fly ash cement paste. *Materials*, *12*(5), 811. https://doi.org/10.3390/ma12050811